Report

Cell Reports

The SLC7A7 Transporter Identifies Microglial Precursors prior to Entry into the Brain

Graphical Abstract

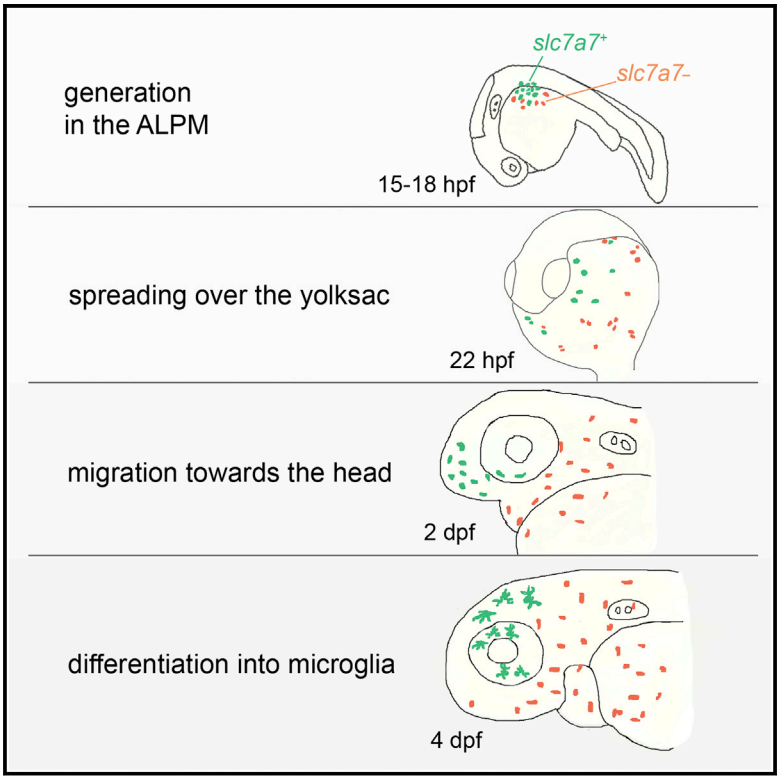

Authors

Federico Rossi,
Alessandra Maria Casano, ...,
Kerstin Richter, Francesca Peri

Correspondence

peri@embl.de

In Brief

This study provides direct experimental evidence for the existence of a microglial sub-lineage among embryonic macrophages. Rossi et al. present a zebrafish mutant that lacks microglia specifically. The underlying gene, *slc7a7*, is expressed in a macrophage subset and is necessary for brain colonization.

Highlights

- Microglia derive from anterior lateral plate mesoderm (ALPM) macrophages
- *slc7a7* is expressed in a subset of macrophages giving rise to microglia
- *slc7a7,* a Leu/Arg transporter, is necessary for microglial brain colonization

Rossi et al., 2015, Cell Reports *11*, 1008–1017
May 19, 2015 ©2015 The Authors
http://dx.doi.org/10.1016/j.celrep.2015.04.028

OPEN ACCESS
CellPress

Cell Reports
Report

The SLC7A7 Transporter Identifies Microglial Precursors prior to Entry into the Brain

Federico Rossi,[1,4] Alessandra Maria Casano,[1,4] Katrin Henke,[2,3] Kerstin Richter,[1] and Francesca Peri[1,*]
[1]Developmental Biology Unit, European Molecular Biology Laboratory (EMBL), Meyerhofstrasse 1, 69117 Heidbelberg, Germany
[2]Department of Genetics, Max-Planck Institute (MPI) for Developmental Biology, Spemannstraße 35–39, 72076 Tübingen, Germany
[3]Present address: Department of Genetics, Harvard Medical School, Orthopaedic Research Laboratories, Boston Children's Hospital, 300 Longwood Avenue, Enders 260.2, Boston, MA 02115, USA
[4]Co-first author
*Correspondence: peri@embl.de
http://dx.doi.org/10.1016/j.celrep.2015.04.028

SUMMARY

During development, macrophages invade organs to establish phenotypically and transcriptionally distinct tissue-resident populations. How they invade and colonize these organs is unclear. In particular, it remains to be established whether they arise from naive equivalents that colonize organs randomly or whether there are committed macrophages that follow pre-determined migration paths. Here, by using a combination of genetics and imaging approaches in the zebrafish embryo, we have addressed how macrophages colonize the brain to become microglia. Identification and cloning of a mutant that lacks microglia has shown that Slc7a7, a Leucine/Arginine transporter, defines a restricted macrophage sub-lineage and is necessary for brain colonization. By taking a photoconversion approach, we show that these macrophages give rise to microglia. This study provides direct experimental evidence for the existence of sub-lineages among embryonic macrophages.

INTRODUCTION

Microglia are the resident macrophages of the brain that play key roles both in development and in several neurodegenerative diseases (reviewed in Saijo and Glass, 2011; Nayak et al., 2014). These cells are morphologically and transcriptionally distinct from other tissue macrophages, such as Langerhans cells in the skin and Kupffer cells in the liver, even though lineage-tracing experiments in mouse have shown that these populations derive from embryonic macrophages (Ginhoux et al., 2010; Schulz et al., 2012; Gomez Perdiguero et al., 2015; reviewed in Derecki and Kipnis, 2013 and Aguzzi et al., 2013). However, it is unclear if these cells derive from naive macrophages that randomly colonize the brain or if this process relies on the existence of pre-committed cells among embryonic macrophages. To date, there are no lineage-specific factors known to be expressed and required prior to brain colonization at early developmental stages. Their identification is fundamental, as it could point to the existence of distinct lineages and to hardwired organ colonization.

Optical transparency and external development have made the zebrafish embryo a powerful model for studying cell lineages in the immune system, including macrophages (Traver et al., 2003; Trede et al., 2004). Here embryonic macrophages were first produced at 20 hours post fertilization (hpf) in the anterior lateral plate mesoderm (ALPM) and later at 30 hpf in a posterior region located in the trunk and called intermediate cell mass (ICM) (Stachura and Traver, 2011; Xu et al., 2012). Using pan-macrophage markers, such as the *macrophage expressed gene 1* (*mpeg1)* and the myeloid transcriptional factor *pU.1*, it has been shown that, at around 2 days post fertilization, some embryonic macrophages invade the brain and differentiate into microglia, as revealed by the expression of *apolipoprotein-E* (*apo-E*) (Herbomel et al., 2001). These microglia are functional and, as does their murine counterpart, engulf apoptotic neurons and respond to brain injuries via ATP/P2Y12 signaling (Peri and Nüsslein-Volhard, 2008; Sieger et al., 2012).

Here we have addressed how microglia colonize the brain by using a combination of genetics and imaging approaches in the zebrafish embryo. In particular, we present a zebrafish mutant that specifically lacks microglia. Cell tracking shows that macrophages are produced and migrate normally, but fail to colonize the brain. Molecular characterization identifies *slc7a7* as the gene underlying this mutation. Using a combination of in situ hybridization (ISH) and live reporters, we show that *slc7a7* is expressed in microglia and, at earlier stages, in a restricted macrophage sub-lineage. Moreover, photoconversion lineage analysis confirms that this population gives rise to the microglia. Thus, this study provides direct experimental evidence that the microglial population in the brain derives from a specific macrophage sub-lineage, thus suggesting the possibility that other organs also might be colonized via targeted migration of defined macrophage progenitors.

RESULTS

Microglia Originate in the ALPM at 22 hpf with No Contribution from the ICM

It has been shown that, in zebrafish, embryonic macrophages are produced in two waves. The first is active between 20 and

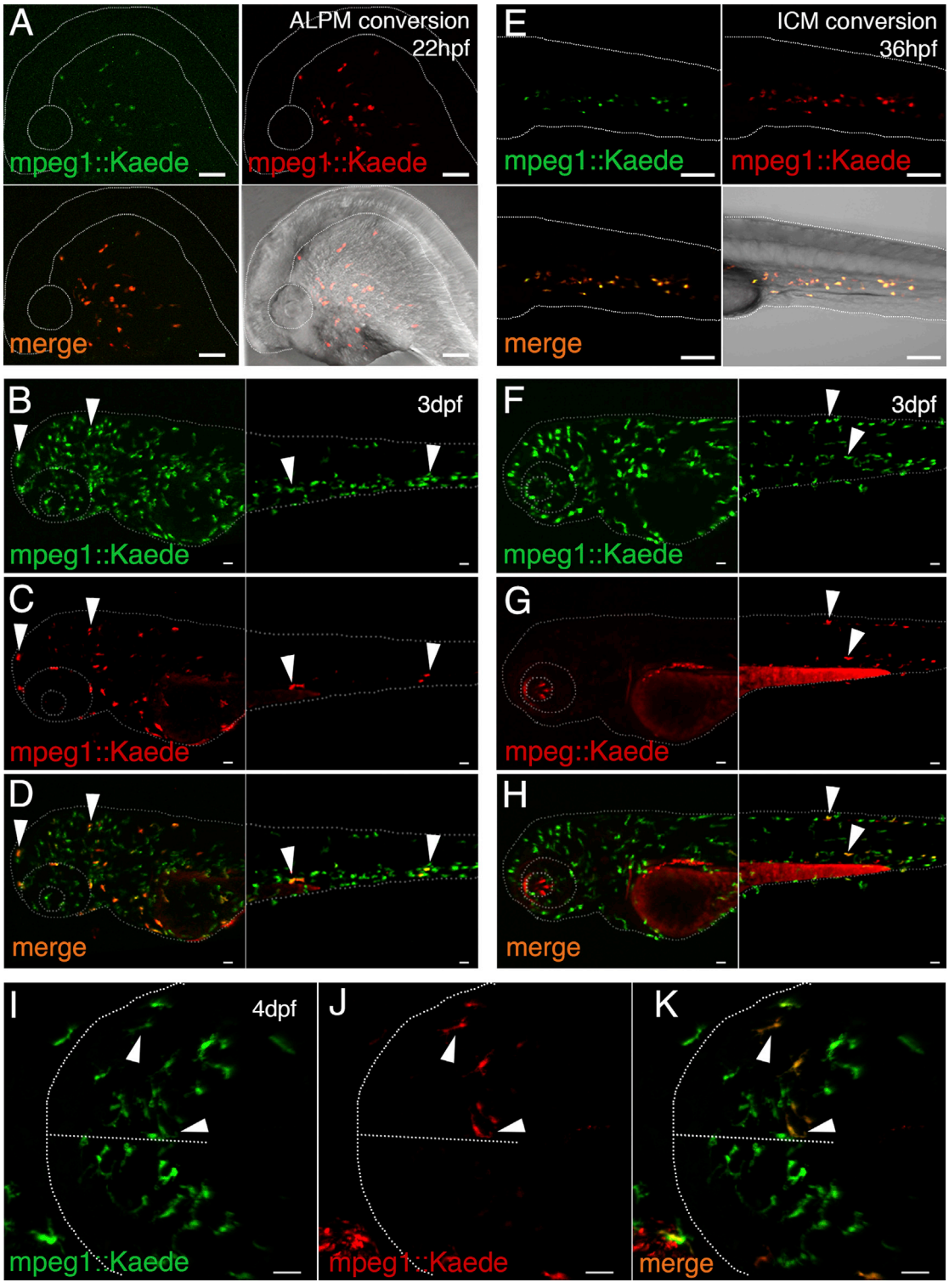

Figure 1. Microglia Derive from ALPM Yolk-Sac Macrophages with No Contribution from the ICM

(A) Photoconversion of ALPM macrophages. Side views of a 22-hpf photoconverted embryo (*mpeg1::Kaede*) are shown (top left, Kaede green; top right, Kaede red; bottom left, overlay of green and red; bottom right, overlay with bright field).

(B–D) Side view shows a 3-day-post-fertilization embryo previously photoconverted at 22 hpf (B, Kaede green; C, Kaede red; D, overlay).

(E) Photoconversion of ICM macrophages. Side views of a 36-hpf photoconverted embryo (*mpeg1::Kaede*) are shown (arranged as in A).

(legend continued on next page)

26 hpf in the ALPM, and the second starts later at 30 hpf in the ICM (Lieschke et al., 2002; Stachura and Traver, 2011; Xu et al., 2012). Thus, we first determined the relative contribution that these two myelopoietic sites have on the establishment of the microglial population. To this aim, we took advantage of the photoconvertible Kaede protein expressed under the control of the macrophage promoter *mpeg1* (*mpeg1::Gal4-UAS::Kaede*; Ellett et al., 2011). This approach allows lineage tracing of cells in vivo, as red fluorescence remains stable over the course of several days and weeks (Ando et al., 2002; Hatta et al., 2006; Dixon et al., 2012; Tomura and Kabashima, 2013).

First, we photoconverted ALPM macrophages at 22 hpf on one side of the embryo only (Figure 1A), and examined these embryos a few days later. These presented many red macrophages along one side of the body and, most importantly, red microglia in one brain hemisphere (16/16 embryos; Figures 1B–1D and 1I–1K). On the contrary, photoconversion of macrophages located over the yolk sac later at 2 days post fertilization failed to label microglia (Figures S1A–S1C), indicating that, at this stage, brain macrophages have already moved away and are no longer located on the yolk sac (Figures S1D–S1F). Interestingly, 4-day-post-fertilization embryos photoconverted at 36 hpf in the ICM region (Figure 1E) presented red macrophages only in the trunk and had no red microglia (6/6 embryos; Figures 1F–1H), suggesting that ICM macrophages do not contribute to the establishment of the microglial population. This is in line with the fact that most anterior macrophages at day 4 are labeled red upon ALPM photoconversion (Figures 1B–1D).

Together these data suggest that microglia derive from anteriorly located macrophages that are produced early during development in the ALPM region, with no contribution from the ICM.

Identification and Characterization of NO067, a Mutant that Lacks Microglia

To understand the mechanism underlying brain colonization by ALPM macrophages, we took a forward genetic approach and searched for mutants that lack microglia. In this way we isolated NO067^{t30713}, a recessive mutant with no microglia in the eyes and brain region, as shown by staining with the microglial marker *apo-E* (Figures 2A and 2B; Figure S2N; Herbomel et al., 2001). Mutant embryos survive until day 7, remain devoid of microglia, and are characterized by the presence of apoptotic corpses within the optic tectum (Figures S2N–S2P). Staining with a wide range of myeloid markers revealed that NO067 maintain circulating monocytes within the brain vasculature (Figures S2C and S2D), macrophages outside the brain (Figures 2C and 2D; Figures S2A and S2B), and neutrophils (Figures S2I–S2K). We also examined Langerhans cells that, like microglia, derive from embryonic macrophages (Hoeffel et al., 2012; Gomez Perdiguero et al., 2015). In mutant embryos, these cells, which are located in the epidermis, have both a normal distribution and branched morphology, indicating that the NO067 phenotype is restricted to the microglial population (Figures S2E–S2H; Lugo-Villarino et al., 2010; Svahn et al., 2013).

To further characterize the NO067 phenotype, we took a quantitative approach using leukocyte- and macrophage-specific transgenic lines. This analysis revealed that there are no defects in myeloid cell production, as at 24 hpf the numbers of leukocytes and macrophages were comparable between wild-type and mutant embryos (Figures 2E–2I). At 2 days post fertilization, during brain colonization, mutants had fewer leukocytes and macrophages in the head region, while in the rest of the body numbers were comparable to wild-type (Figures 2N–2Q). Next, we took advantage of live imaging to assess cell motility and viability among these cells. By comparing speed and track straightness, we found that mutant cells move as sibling counterparts (Figure S3E), also in response to tail injury (Figures S3C, S3D, and S3F; Niethammer et al., 2009). Interestingly, live imaging between 2 and 4 days post fertilization revealed a higher incidence of cell death among mutant macrophages, with these events being mostly located anteriorly, both outside and inside the brain (Figure 2M; Figures S3A and S3B; Movie S1). The resulting cell loss could be detected at the level of total cell counts and might be the reason for lack of microglia at 4 days post fertilization (Figure S2M).

Expression of *slc7a7* in Myeloid Cells Is Required to Establish the Microglial Population in the Brain

High-resolution mapping showed linkage of the NO067 mutation to two makers, SSLP z99015 and SNP zK212K18_2, on LG7. Both showed one recombination event in 1,284 meiosis analyzed, defining an interval of 370 kb. Candidate gene analysis further identified an A to T change in the splice acceptor in intron 4 of *slc7a7*, a gene that shares 73% identity and 91% similarity with the human and murine *slc7a7*, encoding for a solute carrier that mediates the export of Arginine against Leucine (Figure S4A; Sperandeo et al., 2000, 2007). This mutation leads to skipping of the fifth exon resulting in a frameshift and in a premature stop codon (Figures S4B and S4C). Sequencing the genomic region containing the mutation in the two previously identified recombinants confirmed tight linkage of the mutation to the NO067 phenotype. Expression of the *slc7a7* mRNA in macrophages and microglia leads to a significant reduction in the number of homozygous NO067 embryos lacking microglia (Figure 3E). As this rescue is obtained by expressing *slc7a7* in myeloid cells, we conclude that *slc7a7* is required cell autonomously.

Next, we designed a morpholino against *slc7a7*, targeting the fifth exon/intron boundary of the *slc7a7* transcript, and, using specific primers, we confirmed deletion of exon 5 at the molecular level (Figure S4D). At 4 days post fertilization, morpholino

(F–H) Side view shows a 3-day post-fertilization embryo previously photoconverted at 36 hpf (F, Kaede green; G, Kaede red; H, overlay). Red labeling in the eye is due to autofluorescence of the sample.

(I–K) Dorsal view shows a 4-day-post-fertilization embryonic brain previously photoconverted at 22 hpf in the ALPM region (I, Kaede green; J, Kaede red; K, overlay). Dotted line indicates the shape of the brain and the two hemispheres.

White arrowheads indicate Kaede^{+} cells showing both green and red emission. Scale bars for all images, 50 μm. See also Figure S1.

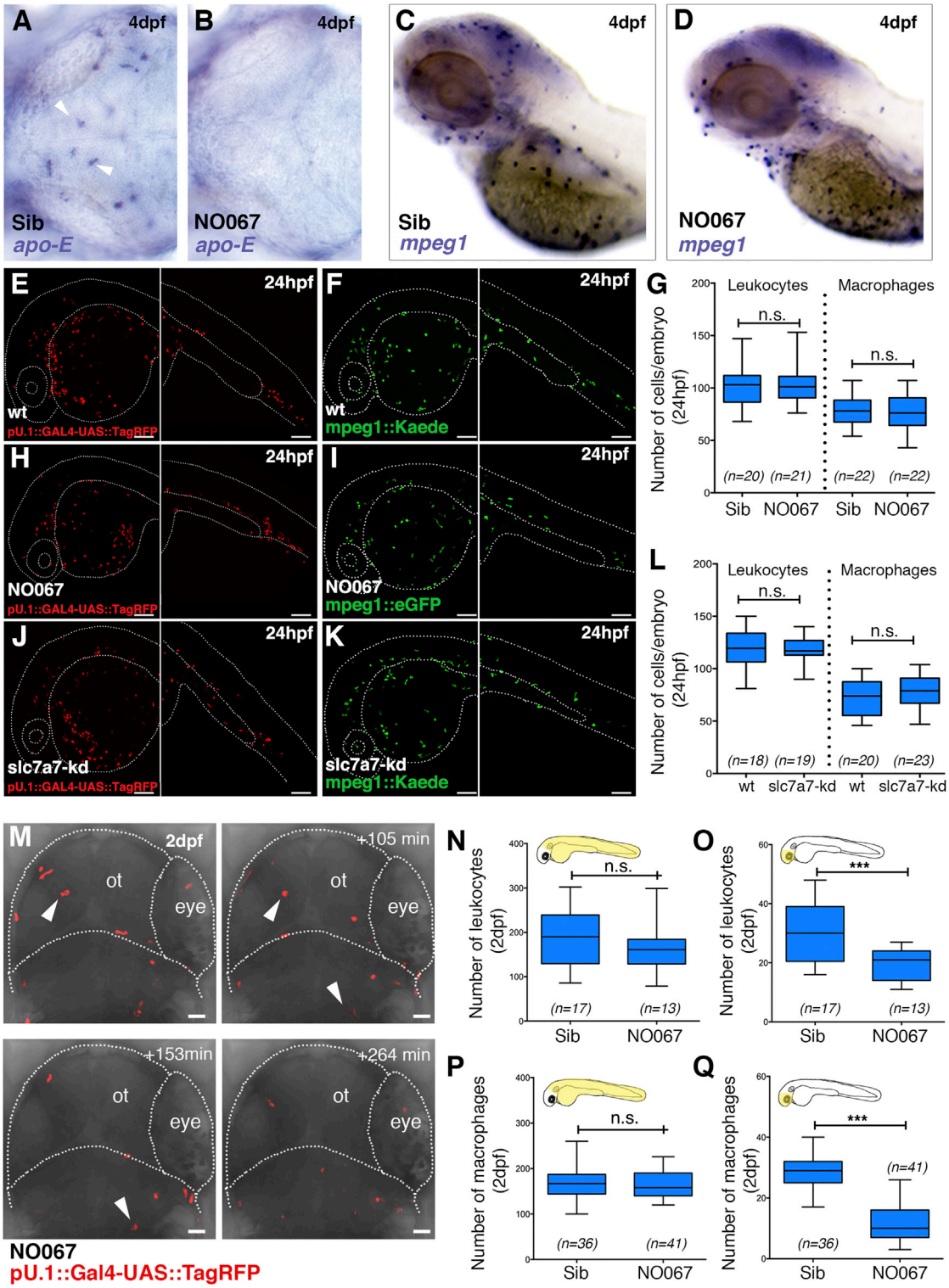

Figure 2. Characterization of the NO067 Zebrafish Mutant

(A and B) WISH for *apo-E* in a sibling (A) and NO067 mutant (B) brain at 4 days post fertilization is shown. White arrows indicate *apo-E*$^{+}$ microglia.

(C and D) WISH for *mpeg1* in a sibling (C) and NO067 mutant (D) embryo at 4 days post fertilization is shown.

(E, H, and J) Lateral view shows a representative *pU1::TagRFP* wild-type (E), mutant (H), and *slc7a7* morphant (J) at 24 hpf.

(F, I, and K) Lateral view shows a representative *mpeg1::Kaede* wild-type (F), *mpeg1::Kaede* morphant (K), and *mpeg1::eGFP* mutant (I) at 24 hpf.

(legend continued on next page)

injections recapitulated the NO067 mutant phenotype with high penetrance (Figures 3A, 3B, and 3H), and already at 2 days post fertilization *slc7a7* morphants lacked *mpeg1*$^+$ macrophages in the eyes and in the brain, even though macrophages were present in the rest of the body (Figures 3C and 3D). Quantifications confirmed what previously was found in *slc7a7* mutants, namely, that *slc7a7* is not required for leukocyte and macrophage cell production, as cell counts at 24 hpf were comparable between injected and un-injected embryos (compare Figures 2E and 2F with Figures 2J and 2K; Figure 2L). Also, at 2 days post fertilization there was correspondence between mutants and morphants, with significantly fewer macrophages and leukocytes in the head region of morpholino-injected embryos (Figures S2Q and S2R).

Taken together these data indicate that *slc7a7* acts cell autonomously within myeloid cells and is necessary to establish the microglial population in the brain.

Slc7a7 Expression Is Restricted to a Myeloid Sub-lineage

As *slc7a7* is required for the establishment of the microglial population, we would expect this gene to be expressed in microglia and in ALPM macrophages. We checked this by ISH and found that *slc7a7* is expressed in the brain in a pattern that resembles that of the microglial marker *apo-E* (compare Figure 3F with Figure 2A). To confirm the identity of these *slc7a7*$^+$ cells in the brain, we knocked down *pU.1*, a transcription factor that is responsible for macrophage and microglia cell production (Lieschke et al., 2002; Rhodes et al., 2005; Peri and Nüsslein-Volhard, 2008). We found no *slc7a7*$^+$ cells in the brain, even though *slc7a7* was still expressed in other non-myeloid domains, such as the gut, pancreas, and head kidney (Figures 3F and 3G; Figures S4F and S4H).

We then asked if this marker also is expressed during brain colonization at earlier stages. Indeed, *slc7a7* starts to be expressed at 22 hpf in cells over the yolk sac (Figure 3I). At later time points, *slc7a7*$^+$ cells are found in an anterior frontal position (Figure 3L). Localization of *slc7a7*$^+$ cells is in line with our previous photoconversion experiments showing that posterior macrophages do not contribute to the establishment of the microglial population (Figures 1E–1H) and that, at 2 days post fertilization, these cells have moved away from the yolk sac region (Figures S1A–S1F). *Slc7a7* expression at early stages is reminiscent of that of other general myeloid markers, such as *pU.1* and *mpeg1*, although it is restricted to fewer cells (compare Figures 3I and 3J with Figures 3L and 3M; Figures 3K–3N). Early expression also was absent in *pU.1* knockdowns, indicating that these cells have a myeloid origin (Figures S4E and S4G).

Together these data indicate that *slc7a7* is expressed in microglia and during early development in a sub-set of anteriorly localized myeloid cells.

Slc7a7$^+$ Cells Are Microglial Precursors

To directly probe the nature of *slc7a7*$^+$ cells, we generated a transgenic line in which the photoconvertible Kaede protein is expressed under the control of the *slc7a7* locus. This transgenic line recapitulates the *slc7a7* ISH pattern and, in particular, it clearly marks the microglial population, as shown by double labeling with *pU.1::Gal4-UAS::TagRFP*, a live reporter that, at 4 days post fertilization, marks microglia in the brain (Figures 4G–4I; Sieger et al., 2012). Most importantly, by crossing the *slc7a7* transgenic line with both *pU.1::Gal4-UAS::TagRFP* and *fms::Gal4-UAS::nfsB-mCherry*, a macrophage reporter (Gray et al., 2011), we found that, at 2 days post fertilization, among TagRFP$^+$ or mCherry$^+$ macrophages, few cells were also *slc7a7*$^+$, confirming that *slc7a7* expression is restricted to a macrophage sub-set (Figures 4A–4F; Figures S4I–S4K).

To directly test if these *slc7a7*$^+$ cells colonize the brain, giving rise to microglia, we photoconverted *slc7a7::Kaede* embryos at 24 hpf, when these cells are produced, and at 44 hpf, during brain colonization. We examined these samples later at 4 days post fertilization and found red microglia in the brain (Figures 4M–4R; Figures S4O–S4Q). The presence of red-labeled microglia resulting from photoconversion at 24 hpf indicates that this cell lineage is specified early, at the time of ALPM macrophage production. Importantly, unconverted samples had no red microglia in the brain (Figures 4J–4L; Figures S4L–S4N). This approach provided direct experimental support for the existence of a macrophage sub-lineage that expresses *slc7a7* and gives rise to the microglia. However, while this clearly shows that the establishment of the microglial population relies on *slc7a7*$^+$ cells, contribution to other lineages cannot be completely excluded.

DISCUSSION

In this study, we used the genetic identification of *slc7a7* to understand principles of microglial brain colonization, and, in particular, we found that *slc7a7* marks a macrophage sub-lineage that gives rise to the microglial population in the brain. What we have not addressed here is the role of *slc7a7* in this process. Interestingly, *slc7a7* joins a growing list of housekeeping genes known to play crucial functions in biological processes such as cell differentiation, survival, and proliferation (Dai et al., 2002; Meireles et al., 2014). In particular, SLC7A5, a transporter for Arginine and Leucine like SLC7A7, constitutes a remarkable example of a housekeeping function that is instrumental for reprogramming T cells (Sinclair et al., 2008).

Although little is known about the mechanism by which these amino acids promote cell differentiation and survival, for SLC7A5 it has been shown that Leucine works as a mediator of the mTOR pathway (Sinclair et al., 2013). However, chemical compounds that have been shown to disrupt the mTOR-signaling pathway in zebrafish do not alter microglial cell numbers (data not shown),

(G and L) Numbers of leukocytes and macrophages in siblings and mutants (G) and wild-type and *slc7a7* morphants (L) at 24 hpf are shown.
(M) Representative time-lapse images show two leukocytes undergoing apoptosis within the head region of a NO067;*pU.1::TagRFP* embryo (white arrowheads). Dotted line indicates the shape of the head and the eye.
(N–Q) Numbers of leukocytes (N and O) and macrophages (P and Q) in siblings and mutants in the head (N and P) and rest of the body (O and Q) at 2 days post fertilization are shown, as indicated in yellow in the schematics. ***$p < 0.0005$, Mann-Whitney test.
Scale bars for all images, 25 μm. Sib, sibling; n, number of embryos. See also Figures S2 and S3 and Movie S1.

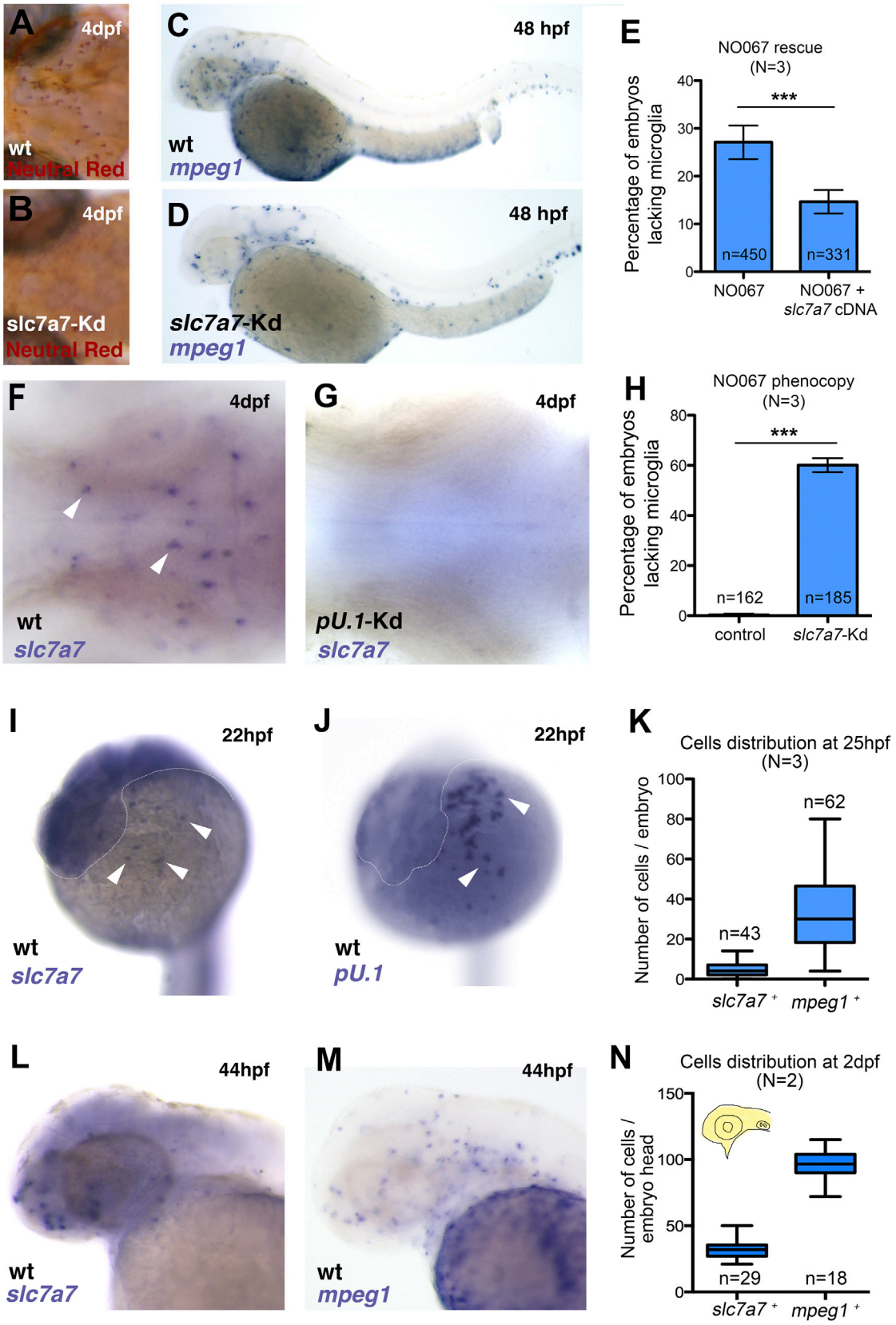

(legend on next page)

suggesting an mTOR-independent role for Slc7a7 in microglial brain colonization. Thus, we speculate that, in the absence of *slc7a7,* the accumulation of Arginine might lead to intracellular nitric oxide (NO) overproduction and induce apoptosis in these cells. Indeed, excess NO has been shown to induce programmed cell death in various cell types via DNA damage and ER stress (Viñas et al., 2006; Mori, 2007; Rudkowski et al., 2004). Interestingly, it has been shown that an increase in *Slc7a7* expression and Arginine transport is characteristic of human monocyte differentiation into macrophages in vitro. Knocking down *Slc7a7* in monocytes leads to Arginine accumulation in these cells (Barilli et al., 2011).

Slc7a7 is the gene mutated in lysinuric protein intolerance (LPI), a human disorder characterized by renal insufficiency as well as neurological and pulmonary complications (Torrents et al., 1999; Borsani et al., 1999; Sperandeo et al., 2008). The finding that this transporter plays a central role in the establishment of microglia is suggestive of the fact that some LPI manifestations could be due to SLC7A7 playing a key role in the establishment of functional tissue-resident macrophages, thus unlocking new approaches for future therapeutical applications. The demonstration that at least one lineage, among tissue-resident macrophages, is specified and identifiable prior to arrival in the host organ opens up a general principle for the existence of tissue-specific macrophage lineages. For example, Langerhans cells, which also in part originate from embryonic macrophages, could be specified prior to arrival in the skin. Interestingly, hardwired positioning of hemocytes, although not described in vertebrates, exists in *Drosophila* where these cells distribute by following Pvf2 and Pvf3, secreted proteins with similarity to the vertebrate PDGF/VEGF (Wood et al., 2006; Parsons and Foley, 2013). Equivalent hardwired guidance also might exist in vertebrates to direct tissue macrophages toward their respective organs during development.

EXPERIMENTAL PROCEDURES

Fish Maintenance and Transgenic Lines

Zebrafish were kept at 26–27°C in a 14-hr light/10-hr dark cycle. Embryos were collected and raised at 28.5°C in E3 solution. To avoid pigmentation, 0.003% 1-phenyl-2-thiourea was added at 1 day post fertilization. Staging of embryos was done according to Kimmel et al. (1995).

The transgenic lines *pU.1::Gal4-UAS::GFP*, *pU.1::Gal4-UAS::TagRFP*, *fms::Gal4-UAS::nfsB-mCherry*, and *mpeg1::Gal4-UAS::Kaede* have been described previously (Peri and Nüsslein-Volhard, 2008; Sieger et al., 2012; Gray et al., 2011; Ellett et al., 2011).

Forward Genetic Screen

N-nitroso-*N*-ethylurea (ENU) was used to induce mutations in male zebrafish according to standard method (Haffter et al., 1996; van Eeden et al., 1999). The screen was conducted at MPI (Tuebingen) as part of "ZF-Models for Human Development and Disease" (http://www.zf-health.org/zf-models). To identify mutants with defects in microglia but no apparent morphological alterations, we incrossed F2 families. The resulting F3 embryos were screened for the presence of microglia at 4 days post fertilization by neutral red assay (Herbomel et al., 2001).

Genetic Mapping

NO067 homozygous mutants were separated from the siblings based on the neutral red phenotype at 4 days post fertilization. We mapped the mutation to LG7 by bulked segregant analysis with the G4 set of sequence-length polymorphism (SSLP) markers, as described previously (Geisler et al., 2007). High-resolution mapping was then conducted using additional polymorphic SSLPs and single nucleotide polymorphisms (SNPs) identified in the linked interval. Sequencing of cDNA of genes in the critical interval identified a deletion of exon 5 in *slc7a7* (GenBank: BC110115.1). Exon skipping was due to a mutation in the splice acceptor of intron 4, shown by sequencing a PCR product obtained by amplifying genomic DNA.

NO067 Phenotype Rescue

For rescuing the NO067 phenotype, we injected a *UAS::slc7a7* construct in clutches of embryos deriving from NO067;*pU.1::Gal4-UAS::GFP* heterozygous mutants. We assayed the rescue by staining microglia with neutral red.

Morpholino Knockdown

Splice morpholino against *slc7a7* (5′-AAAGTGTTTATTACTCACCACAGCC-3′) was purchased from Gene Tools and injected at a concentration of 0.6 mM. The knockdown was validated via RT-PCR. The morpholino against *pU.1* (5′-GATATACTGATACTCCATTGGTGGT-3′, Rhodes et al., 2005) was used at a concentration of 0.5 mM.

Whole-Mount In Situ Hybridization

Whole-mount in situ hybridization (WISH) was performed as described previously (Nüsslein-Volhard and Dahm, 2002). Antisense probes were transcribed for *apo-E*, *mpx*, *mpeg1*, and *slc7a7*.

Kaede Photoconversion

The *mpeg1::Kaede* embryos were photoconverted within a region of interest (ROI) (ALPM, ICM, or yolk sac) using a 10× objective on an Olympus

Figure 3. Slc7a7 Is Expressed in Microglia and a Monocyte Sub-lineage at Early Developmental Stages

(A and B) Neutral red staining shows a representative wild-type (A) and *slc7a7* morphant (B) embryo at 4 days post fertilization, with a lack of microglia in the *slc7a7* morphant brain.

(C and D) WISH for *mpeg1* in a wild-type (C) and a *slc7a7* morphant (D) embryo at 2 days post fertilization. *Slc7a7* morphants lack macrophages in the brain and in the eyes.

(E) Rescue of the NO067 phenotype. Percentages of homozygous *NO067* embryos lacking microglia at 4 days post fertilization, with or without expression of the *UAS::slc7a7* cDNA, are given. Error bars show SEM. ***p < 0.001, Fisher's exact test.

(F and G) WISH for *slc7a7* in the brain of a wild-type (F) and a *pU.1* morphant (G) embryo at 4 days post fertilization (dorsal views). *Slc7a7*$^+$ cells are absent in *pU.1* morphants, indicating that they have a myeloid origin. White arrowheads indicate *slc7a7*$^+$ cells.

(H) Phenocopy of the NO067 phenotype. Percentages of 4-day-post-fertilization embryos lacking microglia in control and *slc7a7* morphant embryos are given. Error bars show SEM. ***p < 0.001, Fisher's exact test.

(I and J) WISH for *slc7a7* (I) and *pU.1* (J) in a wild-type embryo at 22 hpf. White arrowheads indicate *slc7a7*$^+$ and *pU.1*$^+$ cells, respectively. Dotted line indicates the shape of the head.

(K) Numbers of *slc7a7*$^+$ cells and *mpeg1*$^+$ cells at 25 hpf are given.

(L and M) WISH shows 2-day-post-fertilization wild-type embryos stained with *slc7a7* (L) and *mpeg1* (M).

(N) Numbers of *slc7a7*$^+$ cells and *mpeg1*$^+$ cells at 2 days post fertilization are given.

N, number of experiments; n, number of embryos. See also Figure S4.

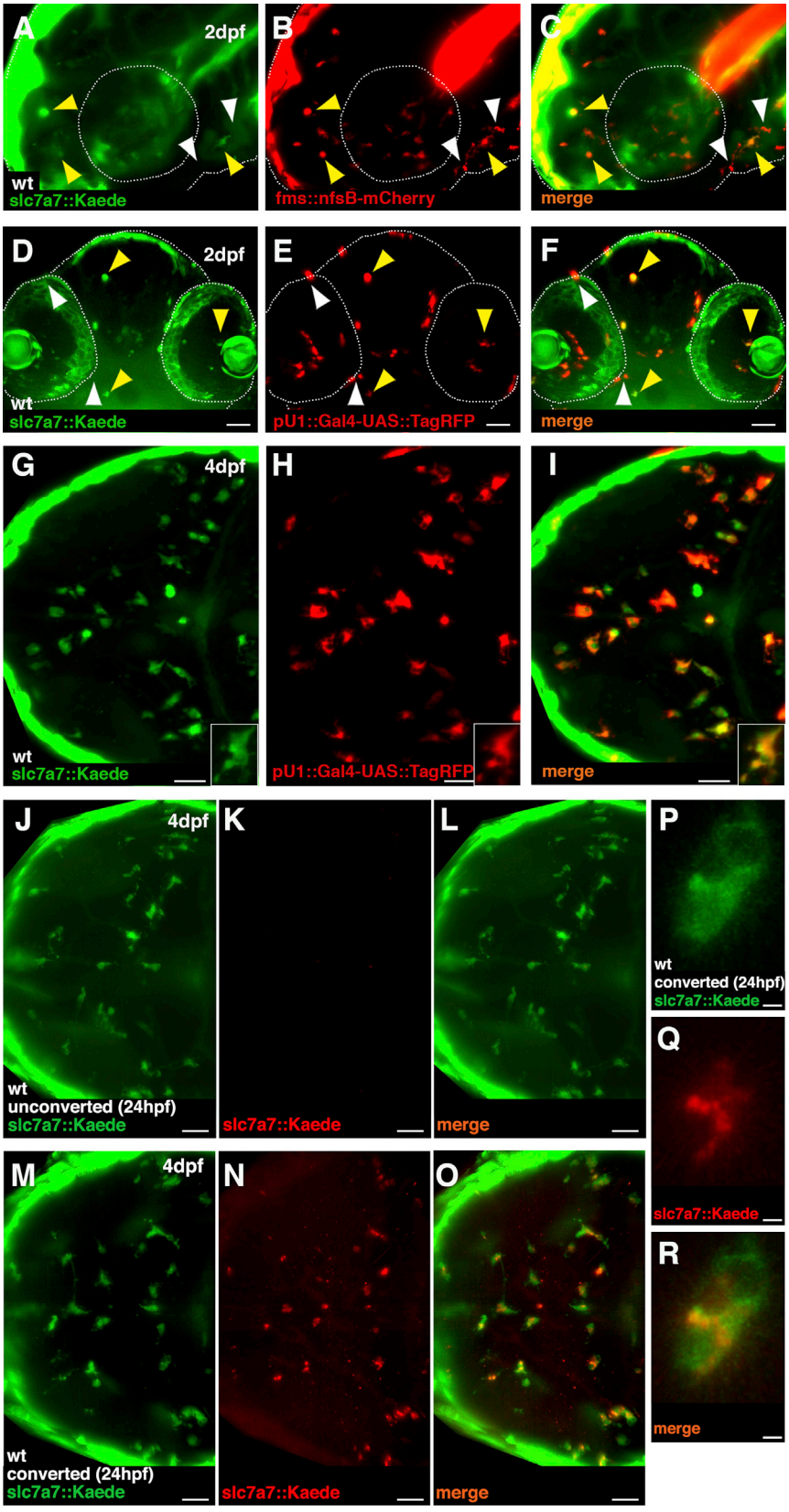

Figure 4. Slc7a7^{+} Cells Give Rise to Microglia in the Brain

(A–C) Lateral view shows a representative *slc7a7::Kaede;fms::nfsB-mCherry* embryo at 2 days post fertilization; *slc7a7*$^{+}$ cells (A, green, *slc7a7::Kaede*), macrophages (B, red, *fms::nfsB-mCherry*), and overlay (C) are shown. Few cells are both *fms*$^{+}$ and *slc7a7*$^{+}$ (yellow arrowheads). White arrowheads indicate *fms*$^{+}$ cells only.

(D–F) Frontal view shows a representative *slc7a7::Kaede;pU.1::TagRFP* embryo at 2 days post fertilization. S*lc7a7*$^{+}$ cells (D, green, *slc7a7::Kaede*), leukocytes (E, red, *pU.1::TagRFP*), and overlay (F) are shown. Few cells are both *pU.1*$^{+}$ and *slc7a7*$^{+}$ (yellow arrowheads). White arrowheads indicate *pU.1*$^{+}$ cells only.

(G–I) Dorsal view shows a *slc7a7::Kaede;pU.1::TagRFP* embryo at 4 days post fertilization. Microglia are both *slc7a7*$^{+}$(G) and *pU.1*$^{+}$ (H), with overlay (I) and a representative microglia (inset) shown.

(J–O) Dorsal view shows a 4-day-post-fertilization *slc7a7::Kaede* embryo not photoconverted (J–L) and photoconverted at 24 hpf (M–O) (Kaede green, J and M; Kaede red, K and N; overlay, L and O).

(P–R) Representative example of a photoconverted microglia is shown.

Scale bars for all images, 25 μm. See also Figure S4.

FV1000 equipped with a 405-nm laser. The following filter sets were used: unconverted Kaede, excitation at 488 nm, emission at 500–550 nm; photoconverted Kaede, excitation at 559 nm, emission at 570–600 nm. *Slc7a7::Kaede* embryos were irradiated with a UV lamp on an Olympus SZX16.

Generation of *slc7a7::Kaede* Transgenic Line, Microscopy, Cell Quantifications and Tracking, Drug Treatments, and Statistical Analysis

For further details regarding materials and methods used in this work, see the Supplemental Experimental Procedures.

SUPPLEMENTAL INFORMATION

Supplemental Information includes Supplemental Experimental Procedures, four figures, and one movie and can be found with this article online at http://dx.doi.org/10.1016/j.celrep.2015.04.028.

AUTHOR CONTRIBUTIONS

K.H. participated in the genetic screen and mapping. F.R. cloned the *slc7a7a* gene. F.R. and A.M.C. designed the study, conducted the experiments, and analyzed the data. K.R. participated in the generation of the *slc7a7::Kaede* line and drug treatments. F.P. designed the study, analyzed the data, and wrote the manuscript with F.R. and A.M.C.

ACKNOWLEDGMENTS

We thank Christiane Nüsslein-Volhard (MPI, Tübingen) for her help and support with this project. The screen was carried out at the MPI (Tuebingen) as part of "ZF-Models for Human Development and Disease" in collaboration with the lab of P. Herbomel (Institut Pasteur, Paris). In particular, we would like to thank Muriel Tauzin for identifying the NO067 mutant. We are grateful to Darren Gilmour, Timm Schlegelmilch, Oksana Breus, and Shinya Komoto for critical reading of the manuscript. We are grateful to the Advanced Light Microscopy Facility (EMBL, Heidelberg) for assistance with microscope imaging.

Received: December 10, 2014
Revised: March 10, 2015
Accepted: April 13, 2015
Published: May 7, 2015

REFERENCES

Aguzzi, A., Barres, B.A., and Bennett, M.L. (2013). Microglia: scapegoat, saboteur, or something else? Science *339*, 156–161.

Ando, R., Hama, H., Yamamoto-Hino, M., Mizuno, H., and Miyawaki, A. (2002). An optical marker based on the UV-induced green-to-red photoconversion of a fluorescent protein. Proc. Natl. Acad. Sci. USA *99*, 12651–12656.

Barilli, A., Rotoli, B.M., Visigalli, R., Bussolati, O., Gazzola, G.C., and Dall'Asta, V. (2011). Arginine transport in human monocytic leukemia THP-1 cells during macrophage differentiation. J. Leukoc. Biol. *90*, 293–303.

Borsani, G., Bassi, M.T., Sperandeo, M.P., De Grandi, A., Buoninconti, A., Riboni, M., Manzoni, M., Incerti, B., Pepe, A., Andria, G., et al. (1999). SLC7A7, encoding a putative permease-related protein, is mutated in patients with lysinuric protein intolerance. Nat. Genet. *21*, 297–301.

Dai, X.M., Ryan, G.R., Hapel, A.J., Dominguez, M.G., Russell, R.G., Kapp, S., Sylvestre, V., and Stanley, E.R. (2002). Targeted disruption of the mouse colony-stimulating factor 1 receptor gene results in osteopetrosis, mononuclear phagocyte deficiency, increased primitive progenitor cell frequencies, and reproductive defects. Blood *99*, 111–120.

Derecki, N.C., and Kipnis, J. (2013). From neurons to microglia, with complements. Nat. Neurosci. *16*, 1712–1713.

Dixon, G., Elks, P.M., Loynes, C.A., Whyte, M.K., and Renshaw, S.A. (2012). A method for the in vivo measurement of zebrafish tissue neutrophil lifespan. ISRN Hematol. *2012*, 915868.

Ellett, F., Pase, L., Hayman, J.W., Andrianopoulos, A., and Lieschke, G.J. (2011). mpeg1 promoter transgenes direct macrophage-lineage expression in zebrafish. Blood *117*, e49–e56.

Geisler, R., Rauch, G.J., Geiger-Rudolph, S., Albrecht, A., van Bebber, F., Berger, A., Busch-Nentwich, E., Dahm, R., Dekens, M.P., Dooley, C., et al. (2007). Large-scale mapping of mutations affecting zebrafish development. BMC Genomics *8*, 11.

Ginhoux, F., Greter, M., Leboeuf, M., Nandi, S., See, P., Gokhan, S., Mehler, M.F., Conway, S.J., Ng, L.G., Stanley, E.R., et al. (2010). Fate mapping analysis reveals that adult microglia derive from primitive macrophages. Science *330*, 841–845.

Gomez Perdiguero, E., Klapproth, K., Schulz, C., Busch, K., Azzoni, E., Crozet, L., Garner, H., Trouillet, C., de Bruijn, M.F., Geissmann, F., and Rodewald, H.R. (2015). Tissue-resident macrophages originate from yolk-sac-derived erythro-myeloid progenitors. Nature *518*, 547–551.

Gray, C., Loynes, C.A., Whyte, M.K.B., Crossman, D.C., Renshaw, S.A., and Chico, T.J.A. (2011). Simultaneous intravital imaging of macrophage and neutrophil behaviour during inflammation using a novel transgenic zebrafish. Thromb. Haemost. *105*, 811–819.

Haffter, P., Granato, M., Brand, M., Mullins, M.C., Hammerschmidt, M., Kane, D.A., Odenthal, J., van Eeden, F.J., Jiang, Y.J., Heisenberg, C.P., et al. (1996). The identification of genes with unique and essential functions in the development of the zebrafish, Danio rerio. Development *123*, 1–36.

Hatta, K., Tsujii, H., and Omura, T. (2006). Cell tracking using a photoconvertible fluorescent protein. Nat. Protoc. *1*, 960–967.

Herbomel, P., Thisse, B., and Thisse, C. (2001). Zebrafish early macrophages colonize cephalic mesenchyme and developing brain, retina, and epidermis through a M-CSF receptor-dependent invasive process. Dev. Biol. *238*, 274–288.

Hoeffel, G., Wang, Y., Greter, M., See, P., Teo, P., Malleret, B., Leboeuf, M., Low, D., Oller, G., Almeida, F., et al. (2012). Adult Langerhans cells derive predominantly from embryonic fetal liver monocytes with a minor contribution of yolk sac-derived macrophages. J. Exp. Med. *209*, 1167–1181.

Kimmel, C.B., Ballard, W.W., Kimmel, S.R., Ullmann, B., and Schilling, T.F. (1995). Stages of embryonic development of the zebrafish. Dev. Dyn. *203*, 253–310.

Lieschke, G.J., Oates, A.C., Paw, B.H., Thompson, M.A., Hall, N.E., Ward, A.C., Ho, R.K., Zon, L.I., and Layton, J.E. (2002). Zebrafish SPI-1 (PU.1) marks a site of myeloid development independent of primitive erythropoiesis: implications for axial patterning. Dev. Biol. *246*, 274–295.

Lugo-Villarino, G., Balla, K.M., Stachura, D.L., Bañuelos, K., Werneck, M.B.F., and Traver, D. (2010). Identification of dendritic antigen-presenting cells in the zebrafish. Proc. Natl. Acad. Sci. USA *107*, 15850–15855.

Meireles, A.M., Shiau, C.E., Guenther, C.A., Sidik, H., Kingsley, D.M., and Talbot, W.S. (2014). The phosphate exporter *xpr1b* is required for differentiation of tissue-resident macrophages. Cell Rep. *8*, 1659–1667.

Mori, M. (2007). Regulation of nitric oxide synthesis and apoptosis by arginase and arginine recycling. J. Nutr. *137* (*6, Suppl 2*), 1616S–1620S.

Nayak, D., Roth, T.L., and McGavern, D.B. (2014). Microglia development and function. Annu. Rev. Immunol. *32*, 367–402.

Niethammer, P., Grabher, C., Look, A.T., and Mitchison, T.J. (2009). A tissue-scale gradient of hydrogen peroxide mediates rapid wound detection in zebrafish. Nature *459*, 996–999.

Nüsslein-Volhard, C., and Dahm, R. (2002). Zebrafish, A Practical Approach (Oxford: Oxford University Press).

Parsons, B., and Foley, E. (2013). The Drosophila platelet-derived growth factor and vascular endothelial growth factor-receptor related (Pvr) protein ligands Pvf2 and Pvf3 control hemocyte viability and invasive migration. J. Biol. Chem. *288*, 20173–20183.

Peri, F., and Nüsslein-Volhard, C. (2008). Live imaging of neuronal degradation by microglia reveals a role for v_0-ATPase a1 in phagosomal fusion *in vivo*. Cell *133*, 916–927.

Rhodes, J., Hagen, A., Hsu, K., Deng, M., Liu, T.X., Look, A.T., and Kanki, J.P. (2005). Interplay of pu.1 and gata1 determines myelo-erythroid progenitor cell fate in zebrafish. Dev. Cell *8*, 97–108.

Rudkowski, J.C., Barreiro, E., Harfouche, R., Goldberg, P., Kishta, O., D'Orleans-Juste, P., Labonte, J., Lesur, O., and Hussain, S.N. (2004). Roles of iNOS and nNOS in sepsis-induced pulmonary apoptosis. Am. J. Physiol. Lung Cell. Mol. Physiol. *286*, L793–L800.

Saijo, K., and Glass, C.K. (2011). Microglial cell origin and phenotypes in health and disease. Nat. Rev. Immunol. *11*, 775–787.

Schulz, C., Gomez Perdiguero, E., Chorro, L., Szabo-Rogers, H., Cagnard, N., Kierdorf, K., Prinz, M., Wu, B., Jacobsen, S.E.J., Pollard, J.W., et al. (2012). A lineage of myeloid cells independent of Myb and hematopoietic stem cells. Science *336*, 86–90.

Sieger, D., Moritz, C., Ziegenhals, T., Prykhozhij, S., and Peri, F. (2012). Long-range Ca^{2+} waves transmit brain-damage signals to microglia. Dev. Cell *22*, 1138–1148.

Sinclair, L.V., Finlay, D., Feijoo, C., Cornish, G.H., Gray, A., Ager, A., Okkenhaug, K., Hagenbeek, T.J., Spits, H., and Cantrell, D.A. (2008). Phosphatidylinositol-3-OH kinase and nutrient-sensing mTOR pathways control T lymphocyte trafficking. Nat. Immunol. *9*, 513–521.

Sinclair, L.V., Rolf, J., Emslie, E., Shi, Y.B., Taylor, P.M., and Cantrell, D.A. (2013). Control of amino-acid transport by antigen receptors coordinates the metabolic reprogramming essential for T cell differentiation. Nat. Immunol. *14*, 500–508.

Sperandeo, M.P., Bassi, M.T., Riboni, M., Parenti, G., Buoninconti, A., Manzoni, M., Incerti, B., Larocca, M.R., Di Rocco, M., Strisciuglio, P., et al. (2000). Structure of the SLC7A7 gene and mutational analysis of patients affected by lysinuric protein intolerance. Am. J. Hum. Genet. *66*, 92–99.

Sperandeo, M.P., Annunziata, P., Bozzato, A., Piccolo, P., Maiuri, L., D'Armiento, M., Ballabio, A., Corso, G., Andria, G., Borsani, G., and Sebastio, G. (2007). Slc7a7 disruption causes fetal growth retardation by downregulating Igf1 in the mouse model of lysinuric protein intolerance. Am. J. Physiol. Cell Physiol. *293*, C191–C198.

Sperandeo, M.P., Andria, G., and Sebastio, G. (2008). Lysinuric protein intolerance: update and extended mutation analysis of the SLC7A7 gene. Hum. Mutat. *29*, 14–21.

Stachura, D.L., and Traver, D. (2011). Cellular dissection of zebrafish hematopoiesis. In The Zebrafish: Cellular and Developmental Biology, Part B, H. Detrich, III and M. Westerfield, eds. (Elsevier), pp. 75–110.

Svahn, A.J., Graeber, M.B., Ellett, F., Lieschke, G.J., Rinkwitz, S., Bennett, M.R., and Becker, T.S. (2013). Development of ramified microglia from early macrophages in the zebrafish optic tectum. Dev. Neurobiol. *73*, 60–71.

Tomura, M., and Kabashima, K. (2013). Analysis of cell movement between skin and other anatomical sites in vivo using photoconvertible fluorescent protein "Kaede"-transgenic mice. In Molecular Dermatology: Methods and Protocols, Methods in Molecular Biology, C. Has and C. Sitaru, eds. (Springer), pp. 279–286.

Torrents, D., Mykkänen, J., Pineda, M., Feliubadaló, L., Estévez, R., de Cid, R., Sanjurjo, P., Zorzano, A., Nunes, V., Huoponen, K., et al. (1999). Identification of SLC7A7, encoding y+LAT-1, as the lysinuric protein intolerance gene. Nat. Genet. *21*, 293–296.

Traver, D., Herbomel, P., Patton, E.E., Murphey, R.D., Yoder, J.A., Litman, G.W., Catic, A., Amemiya, C.T., Zon, L.I., and Trede, N.S. (2003). The zebrafish as a model organism to study development of the immune system. Adv. Immunol. *81*, 253–330.

Trede, N.S., Langenau, D.M., Traver, D., Look, A.T., and Zon, L.I. (2004). The use of zebrafish to understand immunity. Immunity *20*, 367–379.

van Eeden, F.J., Granato, M., Odenthal, J., and Haffter, P. (1999). Developmental mutant screens in the zebrafish. Methods Cell Biol. *60*, 21–41.

Viñas, J.L., Sola, A., Genescà, M., Alfaro, V., Pí, F., and Hotter, G. (2006). NO and NOS isoforms in the development of apoptosis in renal ischemia/reperfusion. Free Radic. Biol. Med. *40*, 992–1003.

Wood, W., Faria, C., and Jacinto, A. (2006). Distinct mechanisms regulate hemocyte chemotaxis during development and wound healing in *Drosophila melanogaster*. J. Cell Biol. *173*, 405–416.

Xu, J., Du, L., and Wen, Z. (2012). Myelopoiesis during zebrafish early development. J. Genet. Genomics *39*, 435–442.